

1  
Abstract # 83

SAND 96-1932C

CONF-970547--1

SAND-96-1932C

## Development of Mo Base Alloys for Conductive Metal-Alumina Cermet Applications

J. J. Stephens, B. K. Damkroger and S. L. Monroe

Materials Joining Department (1833)  
Sandia National Laboratories  
Albuquerque, New Mexico 87185-0367

RECEIVED

MAR 17 1987

OSTI

DISTRIBUTION OF THIS DOCUMENT IS UNLIMITED

ph  
MASTER

### Summary of Paper

A study of thermal expansion for binary Mo-V and ternary Mo-V-Fe/Mo-V-Co alloys has been conducted, with the aim of finding a composition which matches the CTE of 94% alumina ceramic. The overall goal was to identify an alloy which can be used in conductive 27 vol.% metal/73 vol.% alumina cermets. Besides thermal expansion properties, two additional requirements exist for this alloy: (1) compatibility with a hydrogen sinter fire atmosphere and (2) a single phase BCC microstructure. We have identified a ternary alloy with a nominal composition of Mo-22wt.%V-3Fe for use in cermet fabrication efforts. This paper summarizes thermal expansion properties of the various alloys studied, and compares the results with previous CTE data for Mo-V binary alloys.

### Background

Conductive molybdenum/alumina cermets - with typically 50 wt. % molybdenum/50 wt.% alumina, corresponding to 27 vol.% molybdenum/73 vol.% alumina - were developed for high vacuum, high voltage applications in the early 1980's (1,2). The cermet material is either pressed and sintered as a monolithic powder mixture, or poured as a slurry into a green-machined 94% alumina body, followed by a 3 hr./1625°C sinter fire in wet hydrogen. For the cermet/alumina piece parts, relatively simple cylindrical geometries such as conductive cermet feedthroughs were initially fabricated, and no cracks were observed, since the tensile stresses in the alumina were minimized because of the small cermet feature size relative to the surrounding alumina. This was despite the relatively large thermal expansion mismatch between the 94% alumina ceramic and unalloyed molybdenum, as shown in Figure 1. However, when more complicated piece parts were made with larger cermet features, the thermal expansion mismatch between the two materials led to higher tensile stresses in the alumina ceramic, resulting in cracks within the ceramic. For example, the unfired piece part shown schematically in Figure 2a was found to be cracked after firing, and Finite Element Analysis of the residual stresses developed in this piece part indicated that peak tensile stresses as high as 150 MPa were found in the alumina ceramic. As shown in Figure 2b-c, the cracks in the sinter-fired parts appear to initiate in the alumina ceramic immediately adjacent to the corner of the cermet insert.

The present study was initiated as a response to the piece-part cracking problems described above. It was postulated that a binary addition to Mo could be found to increase the thermal coefficient of expansion (CTE) of the alloy so as to match that of the 94% alumina ceramic material. In addition to the CTE requirement, the alloy was required

## DISCLAIMER

This report was prepared as an account of work sponsored by an agency of the United States Government. Neither the United States Government nor any agency thereof, nor any of their employees, make any warranty, express or implied, or assumes any legal liability or responsibility for the accuracy, completeness, or usefulness of any information, apparatus, product, or process disclosed, or represents that its use would not infringe privately owned rights. Reference herein to any specific commercial product, process, or service by trade name, trademark, manufacturer, or otherwise does not necessarily constitute or imply its endorsement, recommendation, or favoring by the United States Government or any agency thereof. The views and opinions of authors expressed herein do not necessarily state or reflect those of the United States Government or any agency thereof.

**DISCLAIMER**

**Portions of this document may be illegible in electronic image products. Images are produced from the best available original document.**

to be single phase BCC and compatible with current sintering and piece part bakeout processes. The requirement of a single phase BCC ensures that no intermediate intermetallic compounds with low melting points are formed. The latter requirement dictates that the Mo-base alloy be compatible with a wet hydrogen atmosphere during the 3 hr. /1625°C cermet sintering treatment, while the vacuum bakeout process requires that the alloying element have low vapor pressure at temperatures up to 1000°C. Although unalloyed Nb has a CTE which is closer to the CTE of the 94% alumina than unalloyed Mo, it cannot be used due to the requirement for hydrogen compatibility.

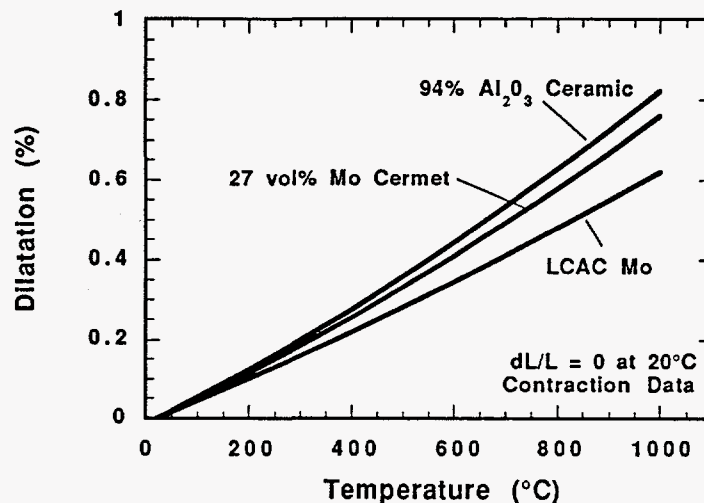
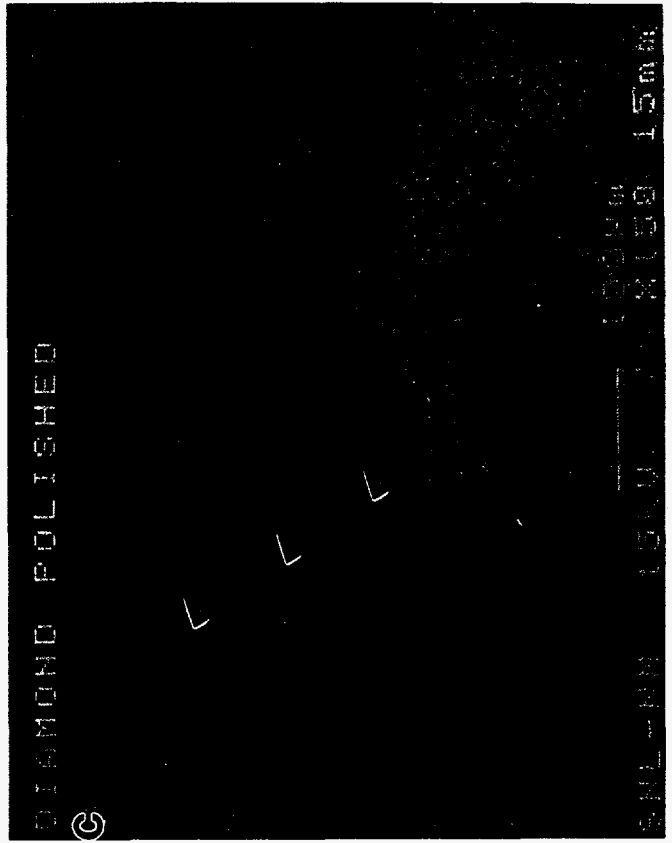
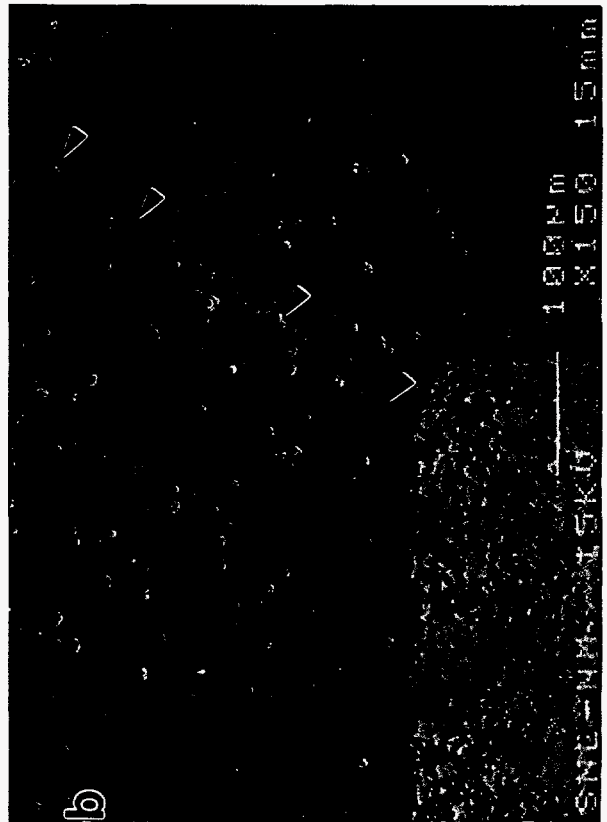
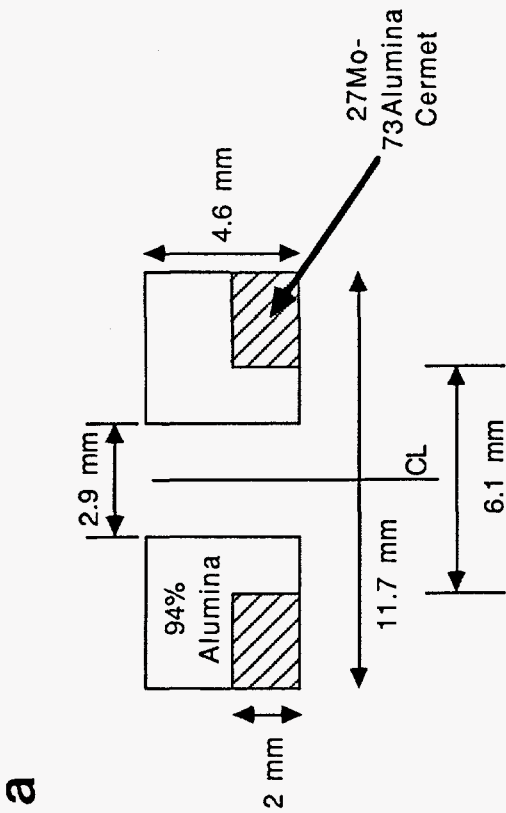


Figure 1. Dilatation plot of thermal expansion data for Low-Carbon, Arc Cast Mo (LCAC Mo), 94% alumina ceramic, and the 27 vol.% Mo/73 vol.% alumina ceramic materials. Data obtained using the dilatometer run in contraction ("on-cooling" mode). The dilatation is adjusted in this plot so that  $dL/L = 0$  at 20°C.

Table 1 Data for average CTE over the temperature range 20-800°C for binary Mo-V alloys from the work of Pridantseva and Solov'eva (4).

<u>Material (wt.%)</u>	<u>Avg. CTE (20-800°C)</u> (10 <sup>-6</sup> /°C)
100 Mo	5.72
90Mo-10V	6.15
85Mo-15V	6.56
78Mo-22V	7.36
62Mo-38V	8.42
56Mo-44V	8.79
43Mo-57V	9.03
33Mo-67V	9.35
20Mo-80V	9.41
100V	9.62

Figure 2. Example of a more complicated cermet/alumina piece part geometry which leads to cracking in the 94% alumina ceramic when it is co-sintered with the 27 vol.% Mo/73 vol.% alumina cermet material. (a) Schematic geometry of the part in the green or unfired condition. (b, c) SEM photos showing cracking in the alumina ceramic. In both photos, the cracks appear to start in the ceramic adjacent to the corner of the cermet insert.



A survey of binary phase diagrams and thermal expansion behavior of binary Mo-X alloy systems (3) suggested that both binary Mo-V and Mo-Cr alloys were good candidates. Previous work (4) on these binary alloys indicated that increases in CTE relative to the properties of unalloyed Mo could be realized. However, due to the relatively high vapor pressure of Cr, it was decided that Mo-Cr alloys would not be compatible with the vacuum bakeout process. For example, the vapor pressure of elemental Cr reaches  $10^{-6}$  and  $10^{-4}$  Torr at the respective temperatures of 838°C and 970°C. Both of these values are incompatible with the use of high vacuum furnace equipment, and thereby eliminated Cr as a candidate alloying element. No such limitation existed with the binary Mo-V alloys, and their use appeared to be feasible, as indicated by the CTE data from ref. 4 shown in Table 1. Thus, a number of binary Mo-V alloys were produced in laboratory batches to permit evaluation of CTE, microstructure and hydrogen compatibility.

### Materials Preparation and Experimental Procedures

Experimental alloys were fabricated as small, cylindrical ingots using a small furnace equipped with a non-consumable tungsten electrode, and a water-cooled copper hearth. Both powder and wire were used as the starting materials, with a total starting weight of 180-200 gms. In order to achieve homogeneity, the buttons were remelted five times, prior to being cast into a cylindrical shape approximately 1.5 cm diameter by 10 cm length. Following fabrication, slices were cut from both the ingot top and bottom, and were examined metallographically. Longitudinal CTE samples were fabricated from sections cut generally from the top of the ingot. Multiple samples blanks were cut using wire EDM from a full cylindrical section of the ingot, and were subsequently ground to final specimen dimensions of 4 x 4 x 25.4 mm.

Dilatation data for all materials discussed in this paper were obtained using a Netzsch dual pushrod dilatometer equipped with silica pushrods and alumina reference material, under a flowing Argon atmosphere. The system error with this setup is less than  $\pm 1\%$ . This experimental setup allowed measurements up to 1000°C; selected alloys were also studied using an alumina push rod setup to 1500°C. These data were consistent with the silica pushrod data but are not included here due to space limitations. Both on-heating and on-cooling data were obtained. The on-heating ramp was 5°C/minute, with a 20 minute hold at the peak (1000°C) temperature. The on-cooling ramps (2°C/min) were typically terminated at 37°C because of the long times needed to cool to room temperature. Where required, extrapolations down to 20°C were made by means of fitting the 37-1000°C dilatation data to a polynomial equation.

Following thermal expansion tests, the CTE samples were metallographically mounted, ground and polished, and quantitative electron microprobe analysis (EMPA) was performed. Probe linescans with points spaced approximately 80  $\mu\text{m}$  apart were run along the length of the CTE samples, with approximately 300 points acquired for each sample. These linescans were averaged to obtain the "mean" alloy compositions as shown in Table 2.

### Characterization of Binary Mo-V Alloys

All of the binary Mo-V alloys studied were found to have a single phase BCC

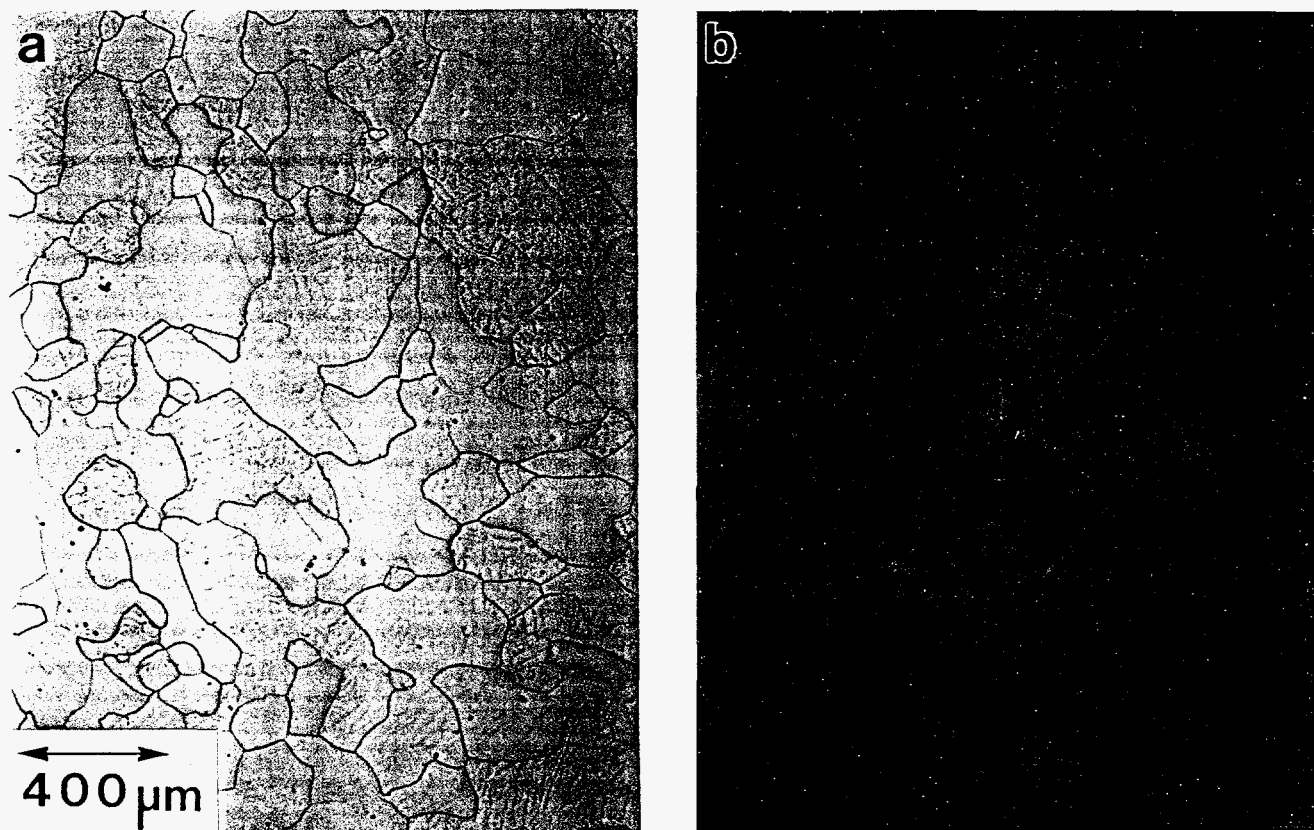


Figure 3. Optical microstructures of the two ingots which were nominally Mo-28V in the as-cast condition. (a) Ingot #1, which was analyzed to have composition of Mo-30.8V. (b) Ingot #2, with a composition of Mo-29.0V.

Table 2 Results of quantitative electron microprobe analyses of CTE samples. Data (wt.%) were obtained from the length of each CTE sample, and are presented as average composition ( $\pm$  standard deviation) based on 300-320 points. Note: the ternary alloys represent avg. of two data sets obtained from adjacent CTE samples.

<u>Nominal Alloy</u>	<u>Vanadium</u>	<u>Molybdenum</u>	<u>Cobalt</u>	<u>Iron</u>
Mo-12.4V	10.91 (1.20)	89.09 (1.43)		
Mo-15.5V	12.61 (1.34)	87.39 (1.67)		
Mo-18V	15.32 (0.91)	84.68 (1.24)		
Mo-28V, #1	30.82 (2.30)	69.18 (2.57)		
Mo-28V, #2	29.00 (1.77)	71.00 (2.04)		
Mo-15V-9Fe	13.89 (1.51)	77.94 (4.52)*	0.00 (0.00)	8.17 (3.32)*
Mo-15V-10Co	13.72 (2.06)	79.06 (11.39)*	7.21 (9.14)*	0.01 (0.01)
Mo-22V-3Fe	21.50 (1.54)	76.10 (2.55)	0.04 (0.028)	2.37 (0.86)
Mo-22V-3Co	20.99 (1.46)	76.56 (2.73)	2.43 (1.29)	0.02 (0.014)

\* Large standard deviations for these two alloys are attributable to their two-phase microstructure.

microstructure. Figure 3 shows the as-cast microstructure for the two highest-Vanadium content alloys studied, with mean compositions determined by electron microprobe analysis of Mo-30.8V and Mo-29.0V, respectively. These results are consistent with published phase diagrams, which indicate a continuous series of solid solution alloys across the Mo-V diagram.

On-heating dilatation data for the various binary Mo-V alloys studied, the 94% alumina ceramic, and unalloyed Low-Carbon Arc-Cast Molybdenum (LCAC Mo) are shown in Figure 4. Clearly, the addition of V to pure Mo leads to a monotonic increase in the thermal expansion of the binary alloys. A summary CTE trend curve for the Mo-V alloys and the 94% alumina ceramic is shown in Figure 5. The CTE data for the binary Mo-V alloys were well fit by a polynomial equation, as shown in Figure 5. These data indicate that a precise fit to the center of the CTE range for the 94% alumina ceramic is obtained at a binary composition of about Mo-32.5V. Tabulated average CTE results for both on-cooling and on-heating data, along with the apparent density of the various alloys, are shown in Table 3.

Table 3. Average thermal expansion (between 37 and 1000°C) for the various alloys studied. Note that both on-cooling and on-heating data are included. The last column contains density measurements acquired from CTE samples.

Nominal Alloy	Actual Composition	Avg. CTE	Avg. CTE	Density (gm/cc)
		On-Cooling (10 <sup>-6</sup> /°C)	On-Heating (10 <sup>-6</sup> /°C)	
LCAC-Mo	100 Mo	6.302	6.262	
Mo-12.4V	Mo-10.9V	6.674	6.803	9.411
Mo-15.5V	Mo-12.6V	6.867	6.903	9.265
Mo-18V	Mo-15.3V	6.895	7.104	9.114
Mo-28V, #2	Mo-29.0V	7.908	8.090	8.522
Mo-28V, #1	Mo-30.8V	8.172	8.244	8.349
Mo-22V-3Fe	Mo-21.0V-2.4Co	7.705*	7.625*	9.005
Mo-22V-3Co	Mo-21.5V-2.4Fe	7.679*	7.702*	9.015
Mo-15V-9Fe	Mo-13.7V-7.2Co	7.930	7.580	-----
Mo-15V-10Co	Mo-13.9V-8.2Fe	7.770	7.640	-----

\* Data represents average of two runs from two separate specimens.

It is also interesting to compare the dilatation results obtained by Prindantseva and Solov'eva (ref. 4) with those of the present study. To do this, all of the binary dilatation data for the binary were fit to a polynomial equation, and the average CTE's between 20° and 800°C were computed. Both on-heating and on-cooling data were included. Figure 6 shows the results of this comparison. Note that there is reasonably good agreement



between the results of the present study and ref. 4, over the range of composition studied. It should be noted that our CTE data for LCAC Mo are about 10% higher than the average CTE for 20-1000°C ( $5.65 \times 10^{-6}/^{\circ}\text{C}$ ) compiled in ref. 6 for unalloyed Mo. We have also consulted producers' data for the 20-1000°C CTE of unalloyed Mo, and have found a value of  $5.8 \times 10^{-6}/^{\circ}\text{C}$  as cited by Plansee (7), while an earlier report from the 1960's cites a value of  $5.82 \times 10^{-6}/^{\circ}\text{C}$  (8). Our results in Table 3 are about 8% higher than these two sources. It is not clear to us why the LCAC-Mo results are higher than other cited literature results for unalloyed Mo.

Extra CTE specimens were used to evaluate the materials' compatibility with the wet hydrogen atmosphere used to sinter-fire the cermet materials. Samples were polished with 1 micron diamond and then carefully weighed using a Mettler Model M5 microbalance. The samples were then subjected to the standard 3 hr./1625°C wet hydrogen sinter-fire treatment, in most cases using furnace runs which were also sinter-firing production cermet piece parts. The results of these tests were expressed in terms of the normalized weight gain (weight gain divided by surface area of the sample), and are presented in Table 4. The "control" sample of LCAC-Mo was found to have a small weight loss. This was presumed to be a result of the reduction of surface oxide during the sinter-fire run. The results for the two binary alloys indicates that there is an increasing tendency for weight gain as the vanadium content is increased. While some of the vanadium oxide formed as an external scale, results discussed in the ternary alloy section indicate that some of the oxidation is internal. These trends in normalized weight gain with respect to increasing V content, led to efforts to develop ternary Mo-V-Co and Mo-V-Fe alloys with slightly reduced V content for the cermet application.

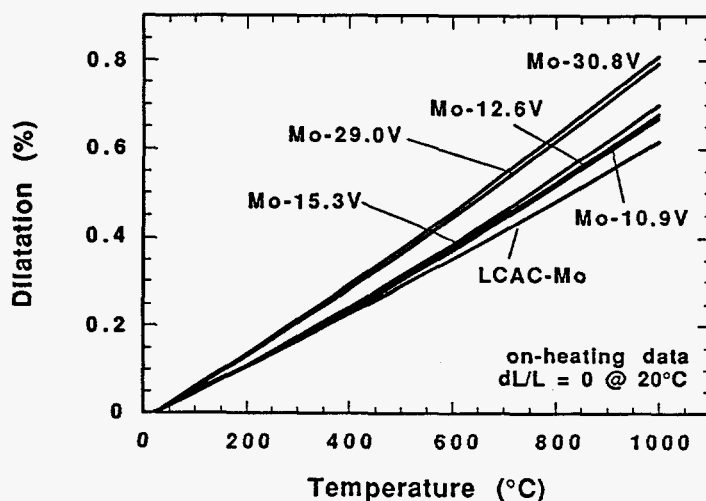


Figure 4. Dilatation data for LCAC-Mo and the various Mo-V alloys studied. The data shown were collected during the on-heating portion of the run, over the temperature range 20-1000°C. The individual data sets were fit to a polynomial fit and adjusted with a constant to impose  $dL/L = 0$  at 20°C.

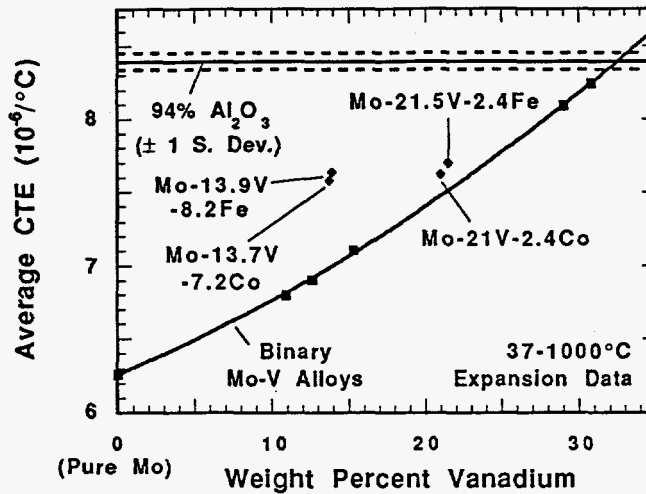


Figure 5. Effect of Vanadium addition to Mo on the average CTE, for on-heating data. In addition to the binary Mo-V alloys, data are included for 5 different lots of the 94% alumina ceramic ( $\pm 1$  standard deviation shown), and the 4 ternary alloys discussed in this paper.

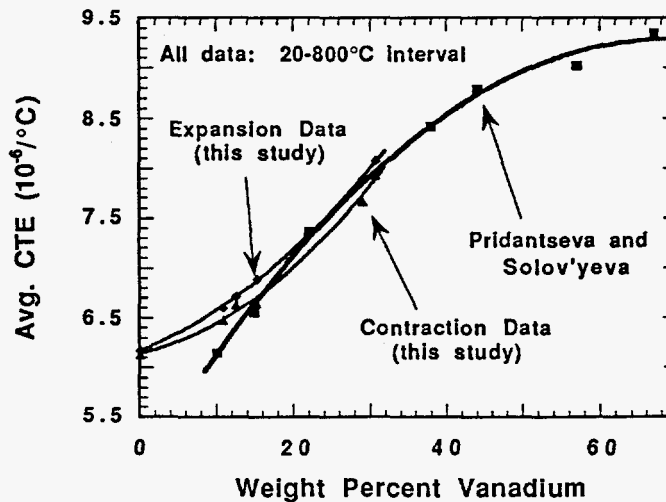


Figure 6. Comparison of CTE data for Mo-V alloys studied by Pridantseva and Solov'eva (ref. 4) with the data generated in this study. Note that all of the CTE data shown in this graph are for the temperature interval 20-800°C.

At the present time, we are in the process of making binary Mo-28V alloy powder using the Plasma Rotating Electrode Process (PREP). The ingot feedstock for the PREP process was a triply melted vacuum arc remelt (VAR) ingot, 12.7 cm in diameter and 17.8 cm long. We intend to use attritor milling to process the coarse PREP powder into finer (~10  $\mu\text{m}$  size) powder which can be used for exploratory cermet sintering experiments.

### Ternary Mo-V-Co and Mo-V-Fe Alloys

In an effort to minimize the amount of vanadium oxide formed during the wet Hydrogen sinter firing treatment, ternary additions of Fe and Co were studied. Both were identified as elements which could increase the CTE of Mo-V binary alloys and afford a good possibility of preserving/promoting hydrogen compatibility. The first two ternary alloys investigated had nominal compositions of Mo-15V-10Co and Mo-15V-9Fe. The thermal expansion of both of these alloys (see Table 3 and Figure 5) does indicate that the Fe and Co additions caused an increase in CTE relative to the comparable Mo-V binary alloy. However, microstructural examination of these alloys, shown in Figure 7, shows that these alloys are not single phase. The extensive second phase observed in the Mo-15V-9Fe alloy - the dark phase shown in Figure 7a - was identified as  $Mo_6Fe_7$  using EMPA, while  $Mo_6Co_7$  was found in the Mo-15V-10Co alloy. Both line compounds are brittle intermetallics, and have relatively low melting points (1550-1600°C), and are not considered suitable for use in cermet materials.

A subsequent examination of the ternary phase stability of the Mo-V-Fe system (6) shows that at 897°C, the maximum amount of Fe that can be added to a 75 wt.% Mo alloy and still remain in the single phase BCC region is ~3.5 wt.% Fe. Thus, two additional alloy ingots were made, with nominal compositions of Mo-22V-3Co and Mo-22V-3Fe. Electron microprobe analysis of CTE samples cut from these ingots indicated actual compositions of Mo-21.0V-2.4Co and Mo-21.5V-2.4Fe (see Table 2). Optical micrographs of both alloys in the as-cast condition, shown in Figure 8, indicate that both alloys are single phase BCC. The on-heating dilatation behavior of these alloys is compared to that of the 94% alumina ceramic and LCAC-Mo in Figure 9. Clearly, the thermal expansion behavior of these two ternary alloys are consistent with the trend curve for binary Mo-V alloys shown in Figure 5, with the Fe or Co additions leading to modest increases in CTE relative to the trend curve prediction for a simple binary Mo-21V alloy.

Additional CTE samples of both the Mo-22V-3Co and Mo-22V-3Fe alloys were also subjected to the 1625°C/3 hr. wet hydrogen sinter firing treatment; the results of those tests are included in Table 4. It would appear, based on comparison with the weight gain results for the 2 binary Mo-V alloys in Table 4, that the Co and Fe additions have little effect on the weight gain behavior. In other words, one would expect a straight binary Mo-

Table 4. Results of hydrogen sinter fire experiments, 3 hrs. at 1625°C, wet hydrogen atmosphere. For all materials except LCAC-Mo, the average normalized weight gain is shown, along with the standard deviation.

Nominal Composition	Actual Composition	Number of Samples	Normalized Wt. Gain (gm/cm <sup>2</sup> )
LCAC-Mo	100 Mo	1	-1.37E-5
Mo-12.4V	Mo-10.9V	3	2.44E-3 ± 7.25E-5
Mo-28V #1	Mo-30.8V	3	9.46E-3 ± 9.79E-6
Mo-22V-3Co	Mo-21.0V-2.4Co	5	5.73E-3 ± 5.95E-4
Mo-22V-3Fe	Mo-21.5V-2.4Fe	4	6.46E-3 ± 3.71E-4

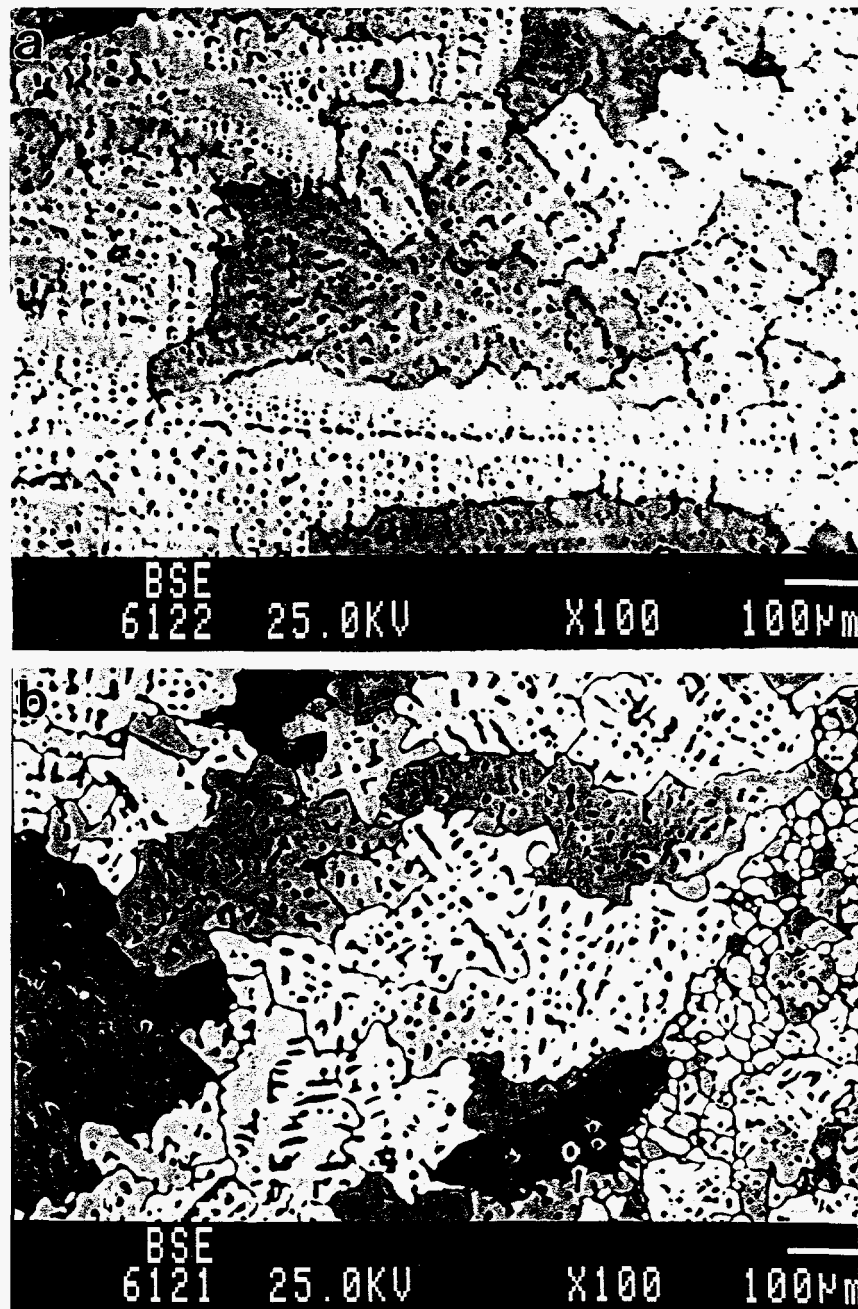


Figure 7. Backscattered electron micrographs of the two-phase ternary alloys. (a) Mo-15V-9Fe alloy. (b) Mo-15V-10Co alloy. The extensive second phase observed in both alloys were analyzed as  $\text{Mo}_6\text{Fe}_7$  and  $\text{Mo}_6\text{Co}_7$ , respectively.

21V alloy to have a normalized weight gain of  $5-6 \times 10^{-3} \text{ gm/cm}^2$  for the standard sinter firing treatment, which is consistent with the range of data observed for the two ternary alloys.

Microstructural examination of the sinter fired Mo-22V-3Fe alloy indicated that some of the weight gain attributable to oxidation of vanadium is internal oxidation. Optical micrographs of a sinter fired sample, shown in Figure 10, indicate the presence of a second phase located near the grain boundaries. Such a second phase was not

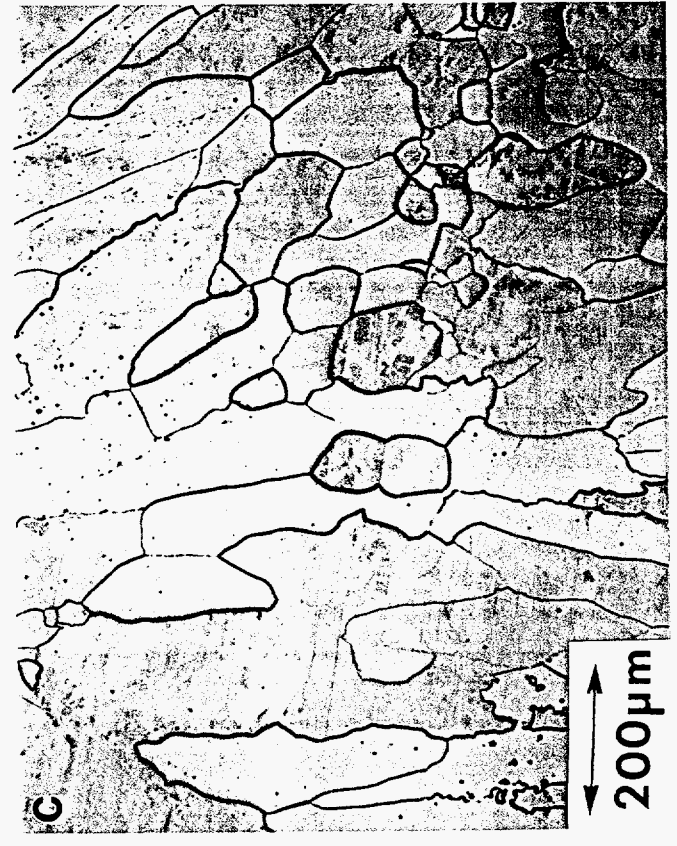
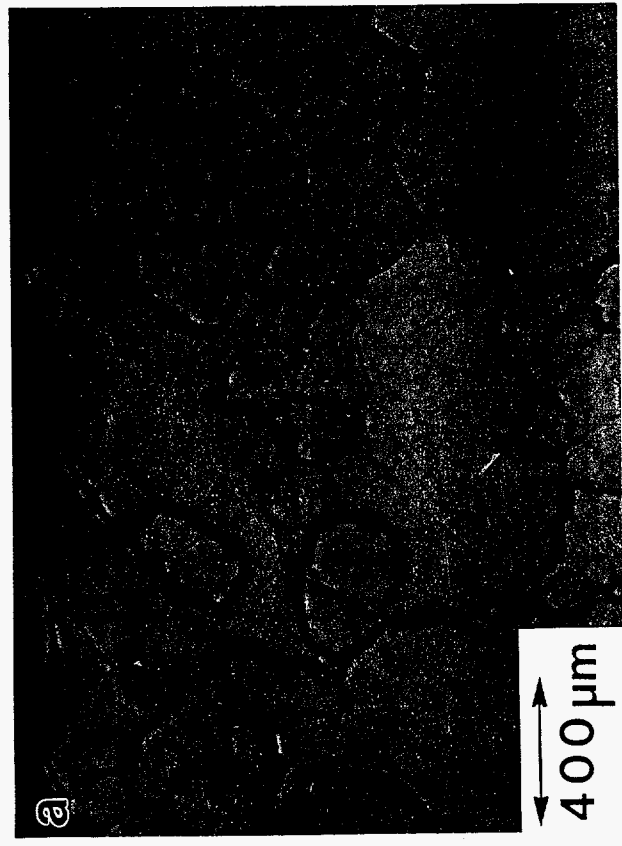
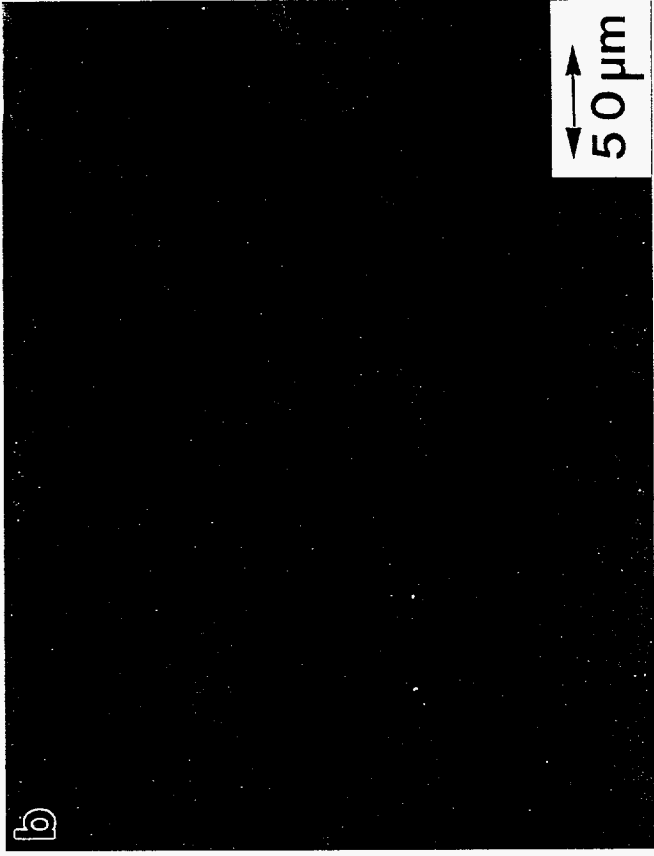


Figure 8. As-cast microstructure of the two single-phase ternaries which were studied. (a) Mo-21.5V-2.4Fe alloy, low magnification micrograph. (b) Higher magnification micrograph of the Mo-21.5V-2.4Fe alloy. (c) Low magnification micrograph of the Mo-21V-2.4Co alloy.

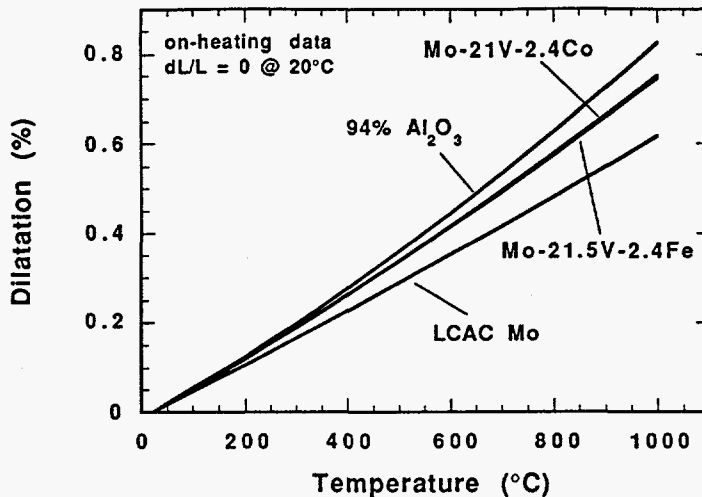


Figure 9. Comparison of dilatation data for LCAC Mo, Mo-21V-2.4Co, Mo-21.5V-2.4Fe and 94% alumina ceramic materials. On-heating data, dL/L has been set to 0 at 20°C.

observed in the as-cast condition and was analyzed using EMPA. Spot EMPA analysis indicated that the second phase is slightly oxygen rich VO, with an average of five points yielding the following results: V  $46.306 \pm 0.229$  at.%, O  $53.508 \pm 0.286$ , Fe  $0.024 \pm 0.022$ , and Mo  $0.164 \pm 0.183$ . A similar second phase indicative of internal oxidation was observed in the sinter fired Mo-22V-3Co alloy. However, the micrographs for this alloy, shown in Figure 11, indicate that the internal oxidation is somewhat more extensive.

On the basis of the sinter firing behavior, and the relative cost of Fe to Co, a decision was made to pursue powder production of the Mo-22V-3Fe alloy. As of this writing, small (100 gm) quantities of this material were produced for us using a mechanical alloying method at the University of California, Irvine. We are currently in the process of pressing this powder into CTE samples, and once the CTE data is generated we will also begin evaluation of cermet sinter firing using this powder.

## Conclusions

This work has confirmed that binary Mo-V alloys do have the potential to match the CTE of 94% alumina ceramic, with a perfect match over the room temperature to 1000°C temperature range expected at Mo-32.5 wt.% V. Modest oxidation of the binary alloys was observed as a result of the 1625°C/3hr. wet hydrogen sinter fire treatment normally used for processing the pure Mo-containing cermets. We have also demonstrated that ternary additions of either 2.4 wt.% Fe or Co can be added to a Mo-21V binary alloy and still retain a single phase alloy, as well as maintaining compatibility with the sinter fire treatment used for cermets.

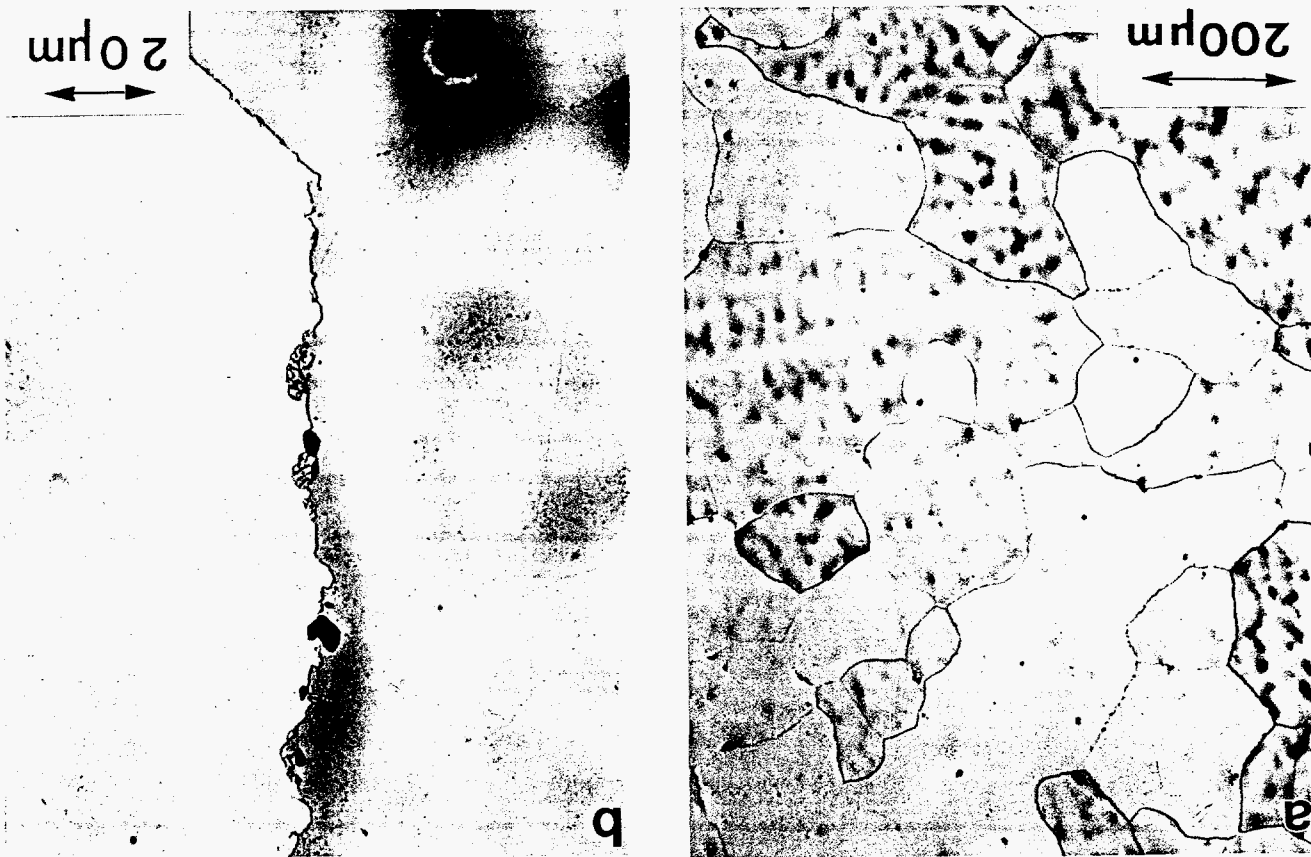


Figure 10. Microstructure of the nominal Mo-22V-3Fe alloy (actual composition = Mo-21.5V-2.4Fe) following 3 hr. anneal at 1625°C in wet hydrogen. (a) Low magnification micrograph. (b) Higher magnification micrograph. The apparent second phase near the grain boundaries was analyzed as vanadium oxide using EMPA.

### Acknowledgements

We would like to acknowledge the help of D. Bencoe, for running the CTE experiments, and P. F. Hlava, for performing the quantitative electron microprobe analysis. The in-kind help of Los Alamos National Laboratory for producing test alloy ingots is acknowledged. The assistance of J. E. Smugeresky at Sandia/California with powder production activities is also appreciated. We thank C. V. Robino of SNL Dept. 1833 for his timely technical review. This work was performed at Sandia National Laboratories, supported by the United States Department of Energy (USDOE) under contract DE-AC04-94AL85000. Sandia is a multiprogram laboratory operated by Sandia Corporation, a Lockheed Martin Company, for the USDOE.

### References

1. D. P. Kramer, K. White and M. D. Kelly, "Effect of Sintering Parameters and Composition on the Resistivity of a Cermet Used as an Electrical Feedthrough," Ceramic Engineering and Science Proceedings, September-October (#9-10), 1982, 3, pp. 512-518.
2. Cermet Insert High Voltage Holdoff For Ceramic/Metal Vacuum Devices, U. S. Patent #4,704,557. Assigned: November 3, 1987.

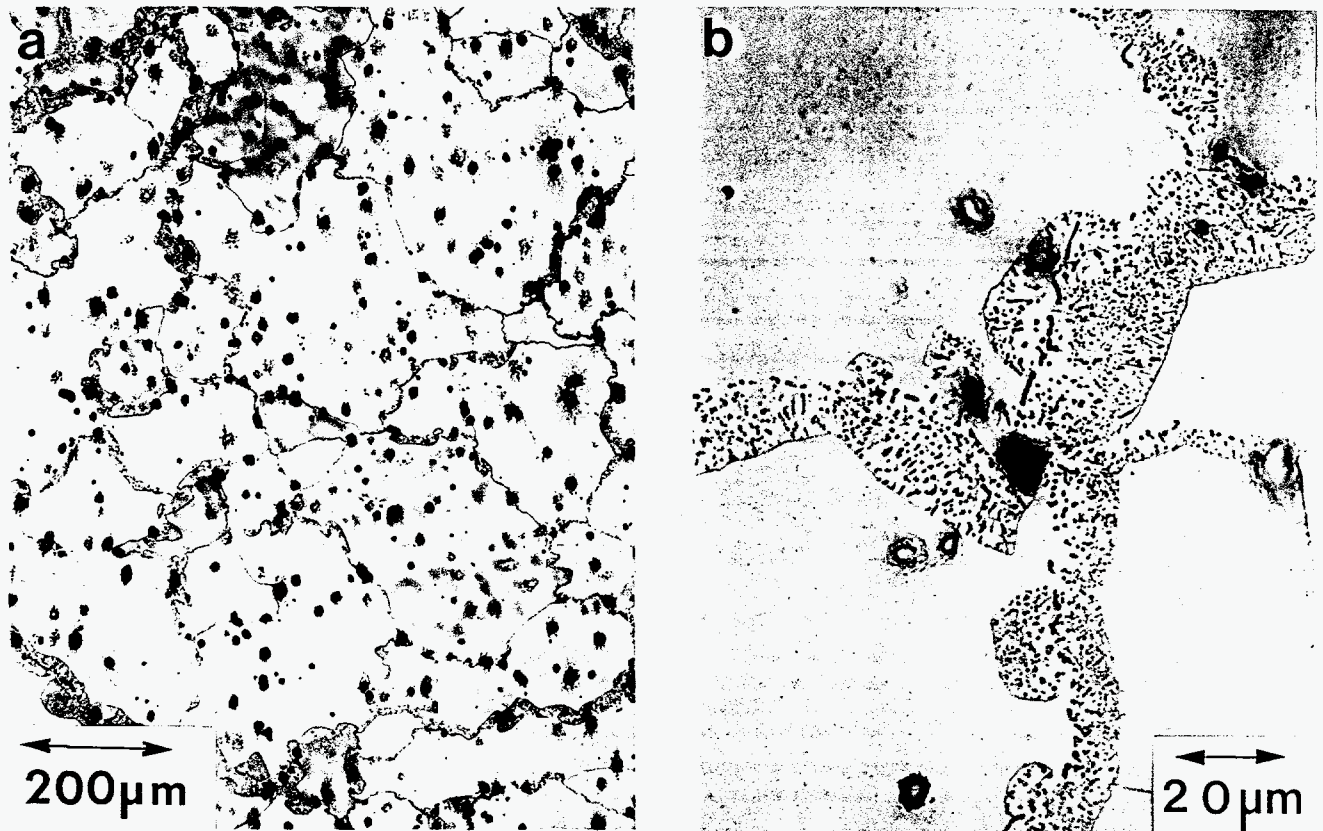


Figure 11. Microstructure of the nominal Mo-22V-3Co alloy (actual composition = Mo-21.0V-2.4Co) following 3 hr. anneal at 1625°C in wet hydrogen. (a) Low magnification micrograph. (b) Higher magnification micrograph. Note that there is a higher density of second-phase vanadium oxide near grain boundaries compared to the sinter fired Mo-22V-3Fe sample in Figure 10.

3. J. J. Stephens, Sandia National Laboratories internal memo, dated March 2, 1995.
4. K. S. Pridantseva and N. A. Solov'eva: *Metal Science and Heat Treatment* 5-6 (May-June, 1966) pp. 478-480.
5. Y. S. Touloukian, R. K. Kirby, R. E. Taylor and P. D. Desai (eds.), Thermophysical Properties of Matter, Volume 12: Thermal Expansion Metallic Elements and Alloys. New York: IFI/Plenum, 1976. p. 208.
6. Metallwerk Plansee: Information on Properties of Molybdenum, 75 page brochure dated March 1992. p. 13.
7. F. F. Schmidt and H. R. Ogden. The Engineering Properties of Molybdenum and Molybdenum Alloys. Columbus, Ohio: Defense Metals Information Center, DMIC Report 190, September 20, 1963. p. A-4.
8. V. Raghavan (ed). Phase Diagrams of Ternary Iron Alloys, Part 6. Calcutta: India Institute of Metals, 1993. pp. 997-1003.